Chemical reactions between cold trapped Ba^+ ions and neutral molecules in the gas phase

B. Roth, D. Offenberg, C. B. Zhang, and S. Schiller
Institut für Experimentalphysik, Heinrich-Heine-Universität Düsseldorf, 40225 Düsseldorf, Germany
(Received 5 August 2008; published 24 October 2008)

Using a laser-cooled ion trapping apparatus, we have investigated laser-induced chemical reactions between cold trapped Ba^+ ions and several neutral molecular gases at room temperature, O_2, CO_2, and N_2O, leading to the production of cold trapped ($\approx$20 mK) BaO^+ ions. The BaO^+ ions were converted back to Ba^+ ions via reaction with room-temperature CO. Reaction rates were determined by employing molecular dynamics simulations. The cold mixed-species ion ensembles produced were used for studying the efficiency of sympathetic cooling, by variation of the ratio of laser-cooled to sympathetically cooled ion numbers. In one extreme case, 20 laser-cooled $^{138}Ba^+$ ions were capable of maintaining the translational temperature of 120 sympathetically cooled barium isotopes ($^{135–137}Ba^+$) and 430 $^{138}Ba^{16}O^+$ molecules at approximately 25 mK.

DOI: 10.1103/PhysRevA.78.042709 PACS number(s): 34.50.−s, 42.50.−p

I. INTRODUCTION

Laboratory studies of gas-phase ion-neutral chemical reactions at low temperatures gained significant interest during the last few years, since they can shed light on the reaction processes occurring in interstellar clouds. One promising route is to investigate chemical reactions between cold atomic and molecular ions trapped in radio-frequency traps and neutral reactants cooled to low translational and sometimes also internal temperatures.

During recent years enormous progress has been made in the production of cold charged and neutral atomic and molecular species, by using a variety of different techniques. For example, cold few-atom neutral molecules can be produced by photoassociation or by using Feshbach resonances in ultracold atomic gases [1–6], by buffer gas cooling in magnetic traps [7], by electrostatic deceleration [8], by cold particle selection and trapping in electric traps [9], and by using superfluid helium droplets [10], among other techniques.

The largest variety of cold species has been obtained in the charged state. Positively charged atomic and molecular ions have been sympathetically cooled using laser-cooled atomic ions in radio-frequency ion traps (see [11–17] for example). Recently, we have shown that two laser-cooled species, Be^+ and Ba^+, are sufficient in order to cool ions with masses ranging from 1 (protons) to 12 400 amu (cytochtrome *c* proteins) to translational temperatures between a few to a few hundred millikelvins [18–20].

Samples of cold trapped atomic or molecular ions open up the possibility to investigate gas-phase ion-neutral chemical reactions with a good accuracy and eventually with resolution of individual quantum states. Because of the experimental challenges, studies of ion-neutral reactions at low temperatures are still very few. A first, and simplest, step is the study of reactions with neutral gas at 300 K. This situation implies collision energies (in the center-of-mass frame) below room temperature if the neutral particles are lighter than the ions. The study of this regime is useful in itself but also for preparing future work on reactions at ultralow energies, e.g., between cold trapped ions and ultracold neutral atomic or molecular gases.

First studies of chemical reactions between cold atomic and molecular ions and room-temperature neutral molecules have been performed. Laser-assisted chemical reactions between crystallized Ca^+ ions and neutral room-temperature O_2 were investigated and reaction rates extracted [21]. The reaction products, CaO^+ ions, in turn, were exposed to room-temperature neutral CO and reacted back to Ca^+ [22]. In another example, the reaction between sympathetically cooled H_3O^+ ions at 10 K and room-temperature NH_3 molecules (leading to the formation of NH_4^+ ions) was studied [23]. Room-temperature chemical reactions, partly laser assisted, were used to produce several light diatomic and triatomic molecular ions at temperatures bellow 20 mK, among them ArH^+, N_2H^+, HO_2^+, BeH^+, as well as H_3^+, H_2^+, and various of their isotopomers. These molecules are interesting for high-precision measurements in fundamental physics and astrochemistry. Reaction coefficients were determined for some processes and compared to Langevin ion-neutral reaction model [24] predictions [19]. In part, the chemical reactions were followed with a resolution down to the single-ion level [19].

In the above studies of ion-neutral reactions only one of the reactants was cold [19,22,25]. Recently, the first investigations of reactive collisions between laser-cooled trapped Ca^+ atomic ions and cold CH_3F molecules at low collision energies ($\geqslant$1 K) were reported and reaction rates were measured [26], opening up a promising route for future investigations. By combining some of the above cooling techniques, it appears feasible in the near future to extend such studies to state-specific ion-neutral reactions with the reactants prepared in pure quantum states and at well-defined collision energies. Measurements of state-specific reactions can provide valuable input for theories of ion-molecule gas-phase chemistry and precise calculations of molecular transition frequencies, offering a unique environment to investigate the quantum-mechanical details of reactive collisions, which usually cannot be observed at higher temperatures.

In this work, we demonstrate an efficient method for the controlled production of heavy heteronuclear molecular ions, BaO^+, based on laser-induced chemical reactions between cold trapped Ba^+ atomic ions and neutral molecular gases, e.g., O_2, CO_2, and N_2O, at room temperature. We thus ex-

tend the work of [21,22] to heavier diatomic ions. The BaO^+ ions cannot be produced directly, e.g., via evaporation from an oven and subsequent electron-impact ionization or photoionization (see, e.g., [14,27]), or using electrospray ionization [16], methods commonly used to create molecular ions in the gas phase.

The formed BaO^+ molecular ions are sympathetically cooled by the laser-cooled Ba^+ ions present in the trap, and, under strong cooling conditions, are embedded in ordered structures, denoted as Coulomb crystals [28,29]. The high degree of localization of the molecular ions in such structures makes them ideal targets for further studies, e.g., of chemical reactions pathways and the determination of total reaction cross sections. For the identification of the particles and the determination of reaction rates we used molecular dynamics (MD) simulations of the ensemble of trapped ions. For consistency, the particle identification based on the simulations was verified by destructive extraction of the particles from the trap and counting as well as by secular excitation mass spectrometry. The simplicity of the method allows for its extension to a large variety of atomic and molecular systems. In addition, by exposing the BaO^+ ions to room-temperature neutral CO molecules a part of them was converted back to Ba^+ ions, thus, showing that further manipulation of the heavy molecular ions produced is possible, similar to the reactions reported for lighter molecular ions [22].

The chemical reactions reported in this work were not studied so far using cold ions in radio-frequency traps. Apart from the conceptual relevance of this work, the systems investigated not only allow us to precisely determine reaction rates by using MD simulations, but also to study some of the properties of cold mixed-species ion plasmas, e.g., the efficiency of sympathetic cooling. This was performed by varying the ratio of laser-cooled (LC) to sympathetically cooled (SC) ions and analyzing the ion crystal translational temperature, via the MD simulations. Furthermore, the accuracy of the reaction rate measurements could be tested by comparison between results obtained via the MD simulations and by direct measurements based on the detection of the Ba^+ ion fluorescence. Good agreement was found between the two methods, at a level which appears sufficient for a precise measurement of reaction coefficients, which can then be compared to predictions from the Langevin ion-neutral reaction model (see [19] for details). The ability to perform measurements with high sensitivity can be important for the measurement of small reaction coefficients which can occur, even for exothermic reactions when the reaction cross sections are small [30]. Furthermore, such measurements, if performed with a resolution down to the single-particle level (see [19]), will enable similar studies of a variety of other reactive processes which were not accessible so far, taking advantage of long storage times possible in our trap apparatus.

II. CHEMICAL REACTIONS

We have studied chemical reactions between laser-cooled, crystallized $^{138}Ba^+$ ions and neutral molecular gases, O_2, CO_2, and N_2O as well as the reaction between sympathetically cooled and crystallized BaO^+ and neutral CO gas:

$$Ba^+ + O_2 \rightarrow BaO^+ + O, \tag{1}$$

$$Ba^+ + CO_2 \rightarrow BaO^+ + CO, \tag{2}$$

$$Ba^+ + N_2O \rightarrow BaO^+ + N_2, \tag{3}$$

$$BaO^+ + CO \rightarrow Ba^+ + CO_2. \tag{4}$$

The reactions in Eqs. (1) and (2) are endothermic by 1 eV and 1.4 eV, respectively [30,32]. Therefore, for our experimental conditions, the translationally cold $^{138}Ba^+$ ions in the $6\,^2S_{1/2}$ ground state do not react with O_2 and CO_2 molecules. However, chemical reactions can proceed when the $^{138}Ba^+$ ions are in the electronically excited $6\,^2P_{1/2}$ or $5\,^2D_{3/2}$ states, at energies of 2.5 and 1.9 eV above the ground state, respectively. This can be achieved using lasers at 493 and 650 nm, required for the (continuous) laser cooling of the Ba^+ ions in the experiments described here (see below for details). The reaction in Eq. (3) is exothermic by 4.9 eV and is expected to proceed with the Ba^+ ions in the electronic ground state or an electronically excited state. Furthermore, the reaction between cold trapped BaO^+ molecular ions and neutral CO molecules is exothermic by 1.4 eV and proceeds with the molecular ions in their electronic ground state [32].

III. EXPERIMENTAL SETUP

A detailed description of our experimental setup has been given previously [15,16]. We use a linear radio-frequency trap for simultaneous storage of both laser-cooled $^{138}Ba^+$ ions and sympathetically cooled molecular ions produced during the chemical reactions. The linear Paul trap consists of four cylindrical electrodes, each sectioned longitudinally into three parts. The overall length of the electrodes is ≈ 10 cm, the central trapping region being 2 cm long. Stable trapping of $^{138}Ba^+$ is achieved with a Mathieu stability parameter $q \approx 0.12$. The transverse oscillation frequency of the trapped particles $\omega_r = (\omega_0^2 - \omega_z^2/2)^{1/2}$, with $\omega_0 = Q V_{\mathrm{rf}}/\sqrt{2} m \Omega r_0^2$. In the longitudinal direction (along the trap axis), the oscillation frequency is given by $\omega_z = (2\kappa Q V_{\mathrm{EC}}/m)^{1/2}$, where V_{EC} is a static potential added to the eight end sections of the electrodes to ensure confinement along the z (trap) axis. The factor $\kappa \approx 1.5 \times 10^{-3}/\mathrm{mm}^2$ is a constant determined by the trap geometry.

The trap is driven at $\Omega/2\pi = 2.5$ MHz, with a peak-to-peak amplitude $2V_{\mathrm{rf}} = 400$ *V* and is enclosed in an ultrahigh-vacuum (UHV) chamber kept at $\approx 5 \times 10^{-10}$ mbar. The chamber is equipped with a leak valve for the controlled introduction of neutral gases, whose partial pressure is controlled by a quadrupole mass analyzer and an ion gauge.

$^{138}Ba^+$ ions are laser cooled on the $6\,^2S_{1/2} \rightarrow 6\,^2P_{1/2}$ transition at 493.5 nm. A repumper laser at 649.8 nm and a magnetic field, applied parallel to the trap axis and of a few gauss magnitude, are required to prevent optical pumping to the metastable $5\,^2D_{3/2}$ state [15]. The two laser beams are linearly polarized in vertical direction and propagate along the trap axis.

For loading the trap, a beam of Ba^+ ions, produced in an UHV evaporator apparatus by evaporation and subsequent ionization of neutral barium atoms is guided through the trap center. During Ba^+ loading the lasers are set to a frequency red detuned from the atomic resonances by several natural linewidths. This ensures, that a part of the Ba^+ ions crossing the beam dissipate a part of their kinetic energy, thus, being trapped and further cooled. For detection, the $^{138}Ba^+$ fluorescence is simultaneously recorded with a photomultiplier tube (PMT) and an intensified charge-coupled device (ICCD) camera.

When strongly cooled, the Ba^+ ion cloud undergoes a phase transition to an ordered state, a Coulomb crystal [29,33]. The produced cold ion ensembles are stable under our conditions [34] and can be stored for many minutes up to several hours in our trap. Such cold plasmas with translational temperatures of a few tens of millikelvins are the starting point for the studies described in this work.

After producing a pure cold Ba^+ ion crystal, neutral gases are introduced to the vacuum chamber at partial pressures in the range $(1-10)\times 10^{-9}$ mbar [corresponding to neutral particle densities in the range $(2.4-24)\times 10^7$ cm^{-3}], using the leak valve. Chemical reactions between the (electronically excited) atomic ions and the neutral molecules lead to the formation of molecular BaO^+ ions, which are sympathetically cooled and crystallized via the Coulomb interaction with the laser-cooled Ba^+ ions. Due to their larger mass-to-charge ratio compared to the laser-cooled $^{138}Ba^+$ ions and the non-laser-cooled (sympathetically cooled) barium isotopes ($^{135-137}Ba^+$ ions), the BaO^+ ions are located outside the Ba^+ crystal body [35]. This leads to a deformation of shape of the Ba^+ ion crystal structure which can be observed in the CCD camera images; see, e.g., Fig. 1. In addition, the Ba^+ ion fluorescence detected via the PMT decreases as the number of Ba^+ ions decreases with time, which also allows for an independent observation of the chemical reactions.

The contents of the trap can be analyzed in several ways [16,19,36]. Resonant secular excitation of the motional resonance of a particular species leads to a drop in the fluorescence intensity of the $^{138}Ba^+$ ions (due to heating induced via ion-ion Coulomb interactions). The ion species can also be identified via destructive techniques based on extraction and counting [16].

Another way to analyze the trap content is via MD simulations [14,19]. The method is described in detail in [37]. It relies on the ability to extract information on different species contained in the ion crystal based on the deformation of shape of the visible Ba^+ crystal structure, observed via the CCD camera. This method can be very sensitive with a resolution down to the single-particle limit, in particular for pure or few-species ion crystals, as observed during this study. The simulations solve Newton's equations of motion of the particles, taking into account the effective (i.e., time-averaged), species-dependent trap pseudopotential, the repulsion forces between all ions, a (constant) light pressure force along the laser beam axis, a viscous damping force representing the laser cooling process, as well as all relevant heating effects present in the trap [16,37]. We do not include micromotion explicitly in the simulations since it does not affect the shape of the ion crystals observed in experiment. Furthermore, for the crystals shown here, the micromotion energy is at 1–2 meV at most, and thus much smaller than the kinetic energy of the neutral room-temperature reactants. Micromotion-related effects, such as rf heating, are nevertheless taken into account phenomenologically in the simulations (see [37] for details). This approach leads to shorter computing times and enables an efficient analysis of the experimental data, without affecting the accuracy of the determination of ion numbers and temperatures and of the variation of shape of the ion crystals during the chemical reactions [37].

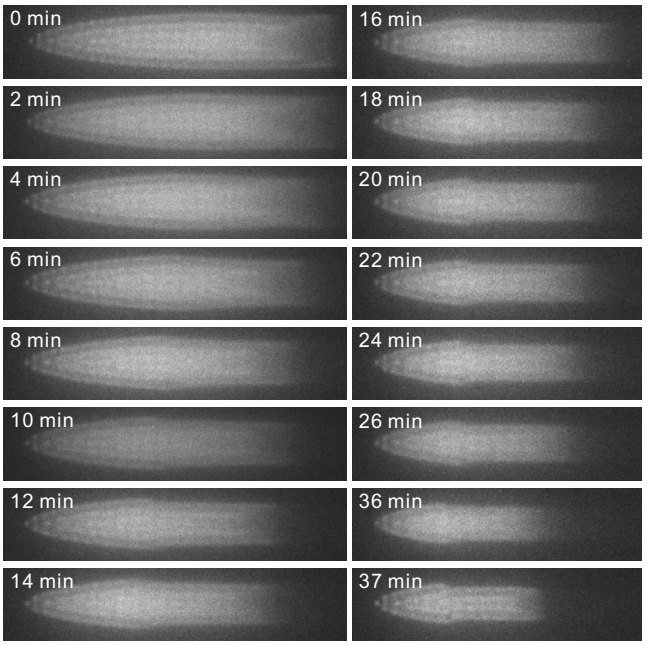

FIG. 1. Time evolution of a Ba^+ ion crystal exposed to neutral O_2 gas at a pressure of 8×10^{-9} mbar. $^{138}Ba^+$ ions are converted to $^{138}Ba^{16}O^+$ ions by chemical reactions. Both cooling lasers at 493 and 650 nm were switched on. Laser beam directions are to the left.

Thus, ion numbers for the laser-cooled ions and the produced molecular ions are obtained as a function of time after the inlet of the neutral reactants to the vacuum chamber. The reaction rate can be deduced from the decrease of the Ba^+ ion number as the chemical reactions proceed or the corresponding increase in the BaO^+ ion number. Similarly, for the reaction between cold BaO^+ ions (which cannot be observed via the CCD camera directly, since they are not laser-cooled and, therefore, do not fluoresce) and neutral CO molecules, the increase of the number of Ba^+ reaction product ions can be monitored via the increase in the Ba^+ fluorescence level or the increase in the number of Ba^+ ions in the CCD crystal image.

For the analysis of the sympathetic cooling efficiency we have varied the ratio between the laser-cooled and sympathetically cooled ions and have analyzed the resulting ion crystal temperature. Note that, usually in addition to the LC $^{138}Ba^+$ ions, there are also other barium isotopes present in the trap (SC $^{135-137}Ba^+$ ions, produced during loading [15]) which are spatially separated from the laser-cooled ions (due to the light pressure force which acts on the latter only) and which are not visible to the CCD camera. They are taken into

account in the simulations for all studies described in this work, since they affect the final temperatures of the ion crystals as well as the crystal shape. The fraction of laser-cooled to non-laser-cooled (SC) barium ions also varies while the chemical reactions proceed, since reaction cross sections are usually different for ground-state or excited-state barium ions (see above).

IV. RESULTS

A. Chemical reactions with residual background gases

In order to accurately determine the reaction rates described above a careful investigation of possible chemical reactions between Ba^+ ions and residual gas molecules present in our trap is required. Under our experimental conditions hydrogen (H_2) and nitrogen (N_2) molecular ions are the main residual gas components. The reaction between ground-state Ba^+ and neutral H_2 is endothermic with a reaction enthalpy of −2.1 eV. It is exothermic when Ba^+ is excited to the $6\,^2P_{1/2}$ electronic state [38]. However, we did not observe this reaction in our trap on time scales of several tens of minutes after inlet of H_2 molecules. This implies a small reaction cross section for this process.

The reaction between Ba^+ ion and N_2 is endothermic and was also not observed in our apparatus. However, small background losses of Ba^+ ions are observed over time scales of several tens of minutes and are attributed to the presence of small amounts of CO_2 in our vacuum chamber. The reaction between ground-state Ba^+ and H_2O molecules, also contained in small amounts in the residual gas, is exothermic with a reaction enthalpy of −0.7 eV [32]. However, it is not observed in our apparatus, probably again due to small cross sections [30]. Also, charge exchange processes between the reactants studied are not possible, according to energetic considerations, and can, therefore, not contribute to any loss mechanism from our trap.

B. Chemical reactions with O_2

In a first step, we have studied the reaction between cold trapped $^{138}Ba^+$ ions excited to the $6\,^2P_{1/2}$ level and neutral O_2 molecules. For all results discussed in this work, the cooling and repumper lasers were tuned to maximum fluorescence, which corresponds to a relative population of the $6\,^2P_{1/2}$ level of 40% (the relative population of the $5\,^2D_{3/2}$ level is 10%). Here, the laser intensities are larger than the saturation intensities for both transitions [31]. Note that, when switching off the repumper laser, all $^{138}Ba^+$ ions are pumped to the $5\,^2D_{3/2}$ level. For this purpose, we have produced a Ba^+ ion crystal containing laser-cooled $^{138}Ba^+$ ions and sympathetically cooled barium ions, $^{135-137}Ba^+$ (upper left panel in Fig. 1). The time evolution of the initial ion crystal during exposure to the neutral molecular gas was observed by using the CCD camera (see Fig. 1). Here, it is obvious that the number of atomic coolants ($^{138}Ba^+$) decreases with time and the ion ensemble changes its shape. In addition to the reduction in size, the outer shells of the crystal are deformed. This is due to the presence of particles with a mass-to-charge ratio larger than that of the atomic coolants, located in the outer regions of the crystal. Since the size of this effect depends on the mass-to-charge ratio of the particles, it can be used for their identification. For the example shown in Fig. 1, the effect can be explained only by the appearance of BaO^+ ion produced via chemical reactions. The ion crystal also contains sympathetically cooled barium ions, which are located in the right part of the crystal (not visible to the CCD camera). Due to light pressure forces, the visible ion shell structure is asymmetric in the axial trap direction (see [15] for details).

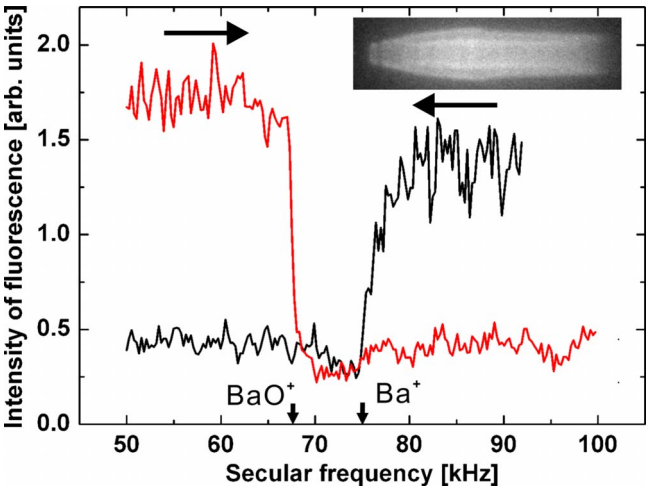

FIG. 2. (Color online) Secular excitation spectra for an ion crystal containing Ba^+ ions, BaO^+ ions (located outside the Ba^+ crystal body), and CO_2^+ ions (located in the dark core of the crystal, not relevant in this work) (see inset). The excitation frequency was swept between 50 and 100 kHz in forward (red curve) and backward (black curve) directions. The method is sufficiently accurate to discriminate between Ba^+ and BaO^+ contained in the crystal.

1. Particle detection and analysis

Particle identification (for this study) was verified using nondestructive secular excitation mass spectrometry (Fig. 2). For this purpose, the radial Ba^+ and BaO^+ modes of oscillation were excited by using an oscillating electric field of variable frequency applied to an external plate electrode (or, alternatively, to the central trap electrodes) (see [15,16] for details). The excitation frequency was swept between 50 and 100 kHz across the Ba^+ and BaO^+ motional resonance frequencies in forward and backward directions, and the induced heating on the particular species was observed, via monitoring the fluorescence intensity of the atomic coolants, using the PMT. The excitation amplitude used heated the ensemble so strongly that the ion crystal was melted when the first species moved into resonance. When scanning from low to high frequency this permitted the measurement of the single-particle BaO^+ frequency at 66 kHz, whereas scanning from high to low frequency allowed for the measurement of the single-particle Ba^+ frequency at 74 kHz. We did not optimize the method in order to resolve the two motional frequencies during a single frequency scan in the forward or backward direction.

Via the MD simulations, ion numbers for the individual species contained in the ensemble can be determined, for

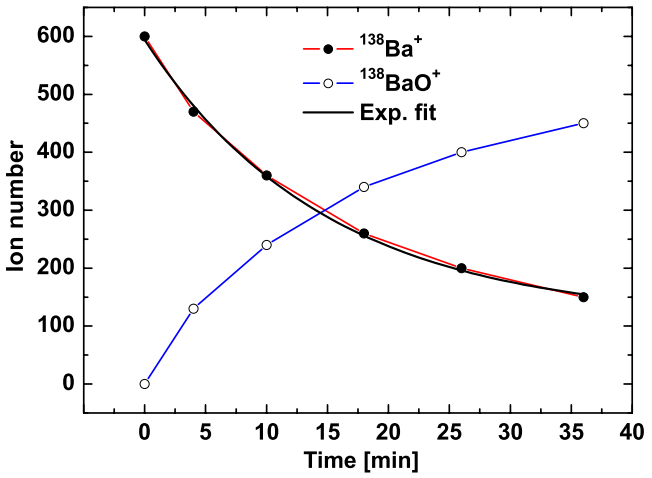

FIG. 3. (Color online) Time evolution of the ion numbers of the $^{138}Ba^+$ and the $^{138}Ba^{16}O^+$ ion ensembles shown in Fig. 1. Each data point in the graph is deduced from a MD simulation of the ion crystal at a particular time. Error bars for the data points (throughout this work) are below 5%. The reaction rate constant Γ for this chemical reaction is obtained by an exponential fit to the Ba^+ ion number decay curve ($\Gamma=0.067\ \mathrm{min}^{-1}$).

each CCD image. For the above reaction study, numbers for $^{138}Ba^+$, $^{135-137}Ba^+$, and $^{138}Ba^{16}O^+$ ions after exposure to O_2 for 0, 4, 10, 18, 26, and 36 min were simulated (see Fig. 3). Typically, for the results shown in this work, the uncertainty in the determination of ion numbers using the simulations is below 5%. The number of $^{138}Ba^+$ ions (full circles) decreases as the number of $^{138}Ba^{16}O^+$ ions (open circles) increases. The number of SC barium isotopes remains nearly constant (not shown in the graph), which is a first indication that ground-state barium ions do not react with O_2 molecules, see discussion below. Initially, the pure barium ion crystal contains approximately 600 $^{138}Ba^+$ ions and 100 SC barium isotopes ($^{135-137}Ba^+$). After exposure to molecular oxygen for 36 min the number of $^{138}Ba^+$ ions decreased to 150, while 450 $^{138}Ba^{16}O^+$ were produced. The above reaction proceeds with a rate constant $\Gamma=0.067\ \mathrm{min}^{-1}$, obtained by exponential fitting the Ba^+ ion number decay curve.

The translational temperature of the ion species contained in the crystal is at $\approx$20 mK (with the temperature of the sympathetically cooled particles being slightly larger than that of the atomic coolants [37]) and does not increase significantly while the fraction of sympathetically cooled ions is increased.

2. *Chemical reactions between ground-state and excited-state* Ba^+ *ions and* O_2

We have studied in more detail whether the chemical reactions proceed with the barium ions in their electronic ground state or in the $5\ ^2D_{3/2}$ excited state. In the first case, an initially pure Ba^+ ion crystal was exposed to neutral O_2 while the cooling and repumper lasers were switched off (Fig. 4). After removing of the O_2 gas and switching on the lasers again the ion ensemble was cooled and recrystallized. The ion numbers were carefully analyzed via the simulations. Neither a loss of Ba^+ ions nor the appearance of BaO^+ ions was observed. In the second case, for a similar ion crystal, the repumper laser was switched off, allowing for optical pumping of the Ba^+ ions to the $5\ ^2D_{3/2}$ excited state. After switching on the repumper laser and removing the O_2 gas from the vacuum chamber we observed a small variation of shape of the barium ion ensemble (see Fig. 5), due to the

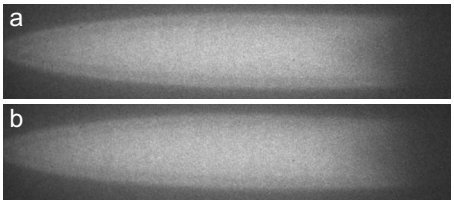

FIG. 4. Chemical reaction between ground state Ba^+ and neutral O_2. After producing an initially pure barium ion crystal (a) the cooling and repumper lasers are blocked for 15 min and the crystal is exposed to O_2. Subsequently, the cooling lasers are unblocked and the ion ensemble recrystallizes (b). No obvious shape deformation is observed nor has the translational temperature of the ion ensemble changed (analyzed using the MD simulations). Thus, chemical reactions between ground-state Ba^+ ions and O_2 do not occur.

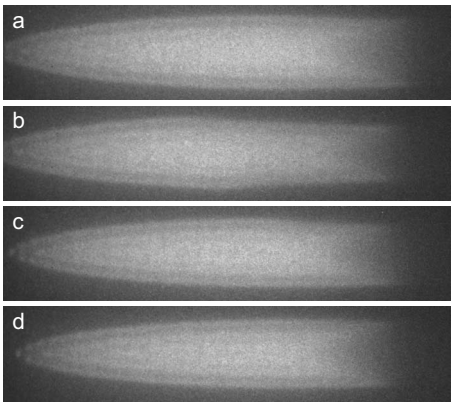

FIG. 5. Chemical reaction between $^{138}Ba^+$ excited to the $5\ ^2D_{3/2}$ state and neutral O_2. (a) Initial barium ion crystal. (b) Barium crystal after exposure to O_2 gas at 8×10^{-9} mbar for 15 min with the repumper laser switched off. All $^{138}Ba^+$ ions were pumped to the $5\ ^2D_{3/2}$ state. BaO^+ ions were formed, leading to a noticeable variation of shape of the LC Ba^+ ion structure [radial squeezing of the LC Ba^+ ion ensemble (visible in the right part of the crystal) and small axial displacement (to the left) of the LC Ba^+ ion ensemble as a whole]. Subsequently, the BaO^+ ions formed were ejected from the trap by secular excitation of their trap modes of oscillation while both lasers were switched off. (c) Ion crystal after switching on the repumper lasers again and one such "cleaning" procedure. A part of the BaO^+ ions was removed, thus reducing the radial squeezing of the crystal compared to (b). (d) Ion crystal after an additional cleaning procedure, finally removing all BaO^+ ions from the trap. As a consequence, the radial squeezing of the crystal vanished and the crystal as a whole was axially displaced to the right [compare positions of the left tips of the crystal in (b), (c), and (d)]. The ion ensemble in (d) contains barium ions only (LC $^{138}Ba^+$ ions and SC $^{135-137}Ba^+$ ions), slightly fewer than the initial ion ensemble in (a). Therefore the tip of the crystal (d) is further to the right than (a).

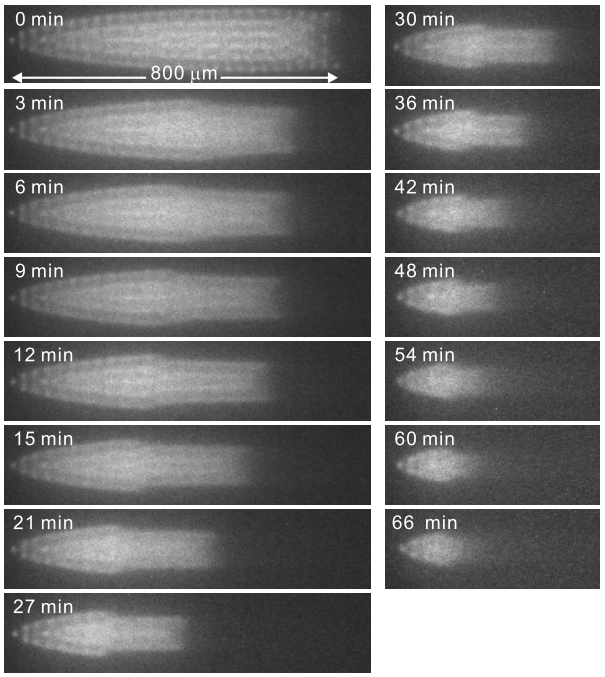

FIG. 6. Time evolution of a Ba^+ ion crystal exposed to neutral CO_2 gas at a pressure of 4×10^{-9} mbar. Both cooling lasers at 493 and 650 nm were switched on. Laser beam directions are to the left.

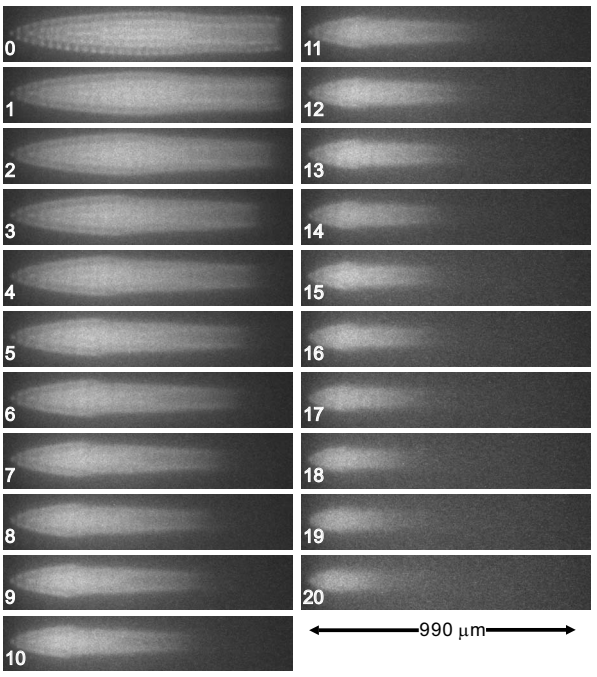

FIG. 7. Time evolution of an initially pure Ba^+ ion crystal exposed to neutral N_2O gas at a pressure of 4×10^{-9} mbar. The time interval between two adjacent CCD images is 10.5 s. The final CCD image was taken about 3.5 min after leaking in N_2O gas.

formation of small amounts of BaO^+ ions. Consequently, the Ba^+ ion number decreased slightly. However, the reaction rate constant determined using the simulations is much smaller compared to the case when the lasers are switched on, even for much higher O_2 partial pressures, and does not contribute significantly to the reaction rate constants determined.

C. Chemical reactions with CO_2 and N_2O

We have also studied the chemical reactions between laser-cooled Ba^+ ions and room-temperature CO_2 (Fig. 6) and N_2O molecules (Fig. 7). The corresponding reaction rate constants were determined in the same way as described above (Figs. 8 and 9, respectively), via the MD simulations.

For the CO_2 case, the original barium ion crystal contains about 450 $^{138}Ba^+$ ions and 120 SC barium isotopes. The $^{138}Ba^+$ ion number decreases to about 260 during exposure to the neutral reactants for about 9 min, and the $^{138}Ba^{16}O^+$ ion number increases from 0 to about 190. Again, the number of SC barium isotopes and the ion crystal temperature ($\approx$20 mK) remain nearly constant during the reaction. The reaction rate constant is $\Gamma=0.062$ min^{-1}, comparable to the constant determined for the O_2 case at a larger oxygen partial pressure (4×10^{-9} mbar for CO_2 compared to 8×10^{-9} mbar for O_2). No reaction products were observed when either one or both laser beams were switched off, showing that the chemical reaction proceeds with the Ba^+ ions excited to the $6\,^2P_{1/2}$ electronic state only.

For the case of N_2O and comparable experimental conditions, the reaction rate constant ($\Gamma=0.016$ s^{-1}) is much larger compared to the examples discussed before. However, the number of SC barium isotopes remains constant during exposure to the N_2O (here, the exposure time of $\approx$10 min is shorter compared to the other examples discussed). Also, the reaction of $^{138}Ba^+$ in the electronic ground state (when the cooling lasers are off) was not observed. These observations

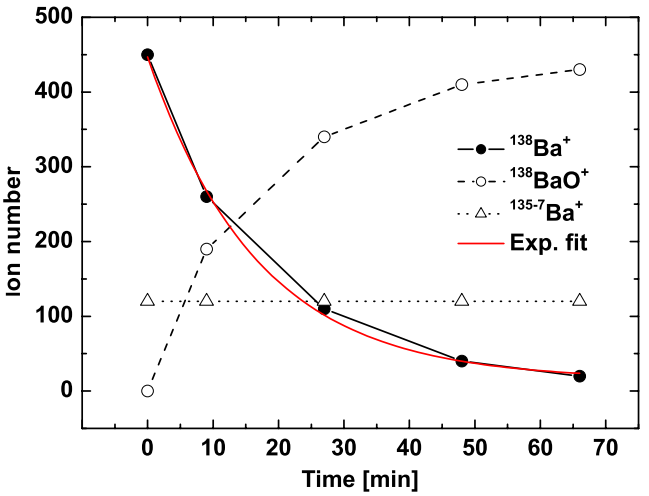

FIG. 8. (Color online) Time evolution of the numbers of the LC $^{138}Ba^+$, the SC $^{135-137}Ba^+$ isotopes, and the $^{138}Ba^{16}O^+$ ion ensembles shown in Fig. 6. ^{138}Ba ions react with CO_2 gas and generate the same amount of $^{138}Ba^{16}O^+$ ions, the SC barium isotopes do not react with the molecules. The reaction rate constant Γ for this chemical reaction is obtained by an exponential fit to the Ba^+ ion number decay curve ($\Gamma=0.062$ min^{-1}). Reactions between ground-state Ba^+ ion and CO_2 and between Ba^+ ions excited to the $5\,^2D_{3/2}$ state and CO_2 were not observed.

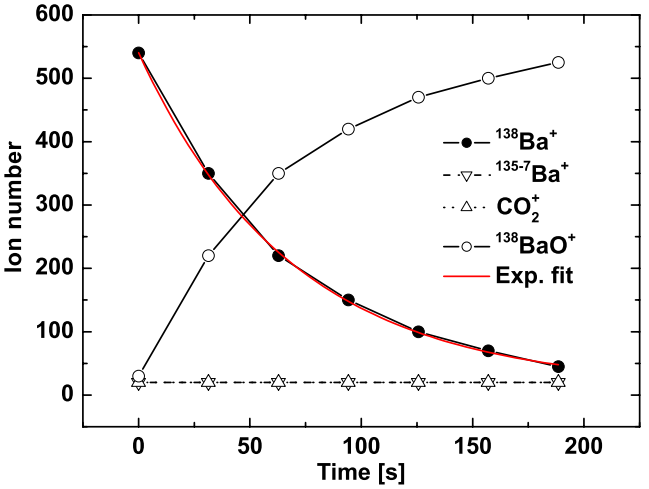

FIG. 9. (Color online) Time evolution of the numbers of the LC $^{138}Ba^+$, SC $^{135-137}Ba^+$ isotopes, CO_2^+, and $^{138}Ba^{16}O^+$ ion ensembles shown in Fig. 7. $^{138}Ba^+$ ions react with NO_2 gas and generate $^{138}Ba^{16}O^+$ ions, whereas the SC barium isotopes as well as CO_2^+ ions generated during loading do not react with the neutral molecules. The reaction rate constant Γ for this chemical reaction is obtained by exponential fitting to the Ba^+ ion decay curve ($\Gamma = 0.016\ s^{-1}$).

may indicate that although the reaction is exothermic even with the Ba^+ ions in the ground state, activation energy is required in order to overcome a reaction barrier and to induce the reaction.

In order to test the accuracy of the measurement and analysis technique described we compare the results from MD simulations with results obtained by direct observation of the atomic coolant fluorescence while the chemical reactions proceed (Fig. 10). Within the experimental resolution, we obtain essentially the same result for the Ba^+ ion number decay and the reaction rate constant deduced. Note, that in order to determine reaction rates and reaction rate coefficients the chemical reactions described above need to be studied as a function of the excited level Ba^+ population and of the partial pressure of the neutral reactants. The corresponding Langevin coefficients can then be deduced by normalizing the reaction coefficients to the neutral reactant particle number density and the excitation level, as demonstrated in [19]. This is, however, well beyond the scope of this work and may be studied systematically in future investigations.

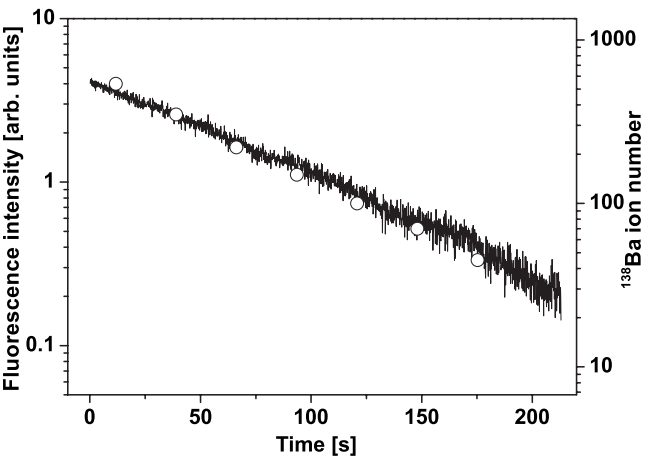

FIG. 10. Comparison between different detection techniques. Time evolution of the fluorescence intensity of the Ba^+ ion crystal shown in Fig. 7 (exposed to neutral N_2O gas at a pressure of 4×10^{-9} mbar). The reaction rate deduced from the Ba^+ ion number decay curve (open circles, see also Fig. 9) agrees well with the decay rate constant obtained from the fit to the fluorescence decay curve.

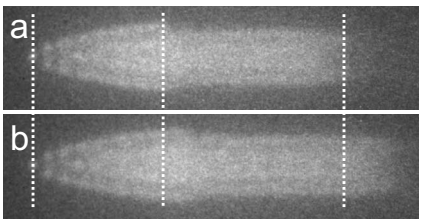

FIG. 11. Chemical reaction between cold trapped BaO^+ ions and neutral CO gas at a pressure of 1×10^{-8} mbar. (a) CCD image of a two-species ion crystal containing Ba^+ and BaO^+ ions. The latter were produced by chemical reactions Ba^+ ions and neutral CO_2 gas (see Fig. 6). (b) CCD image of the ion ensemble after leaking in CO gas for 10 min. The number of Ba^+ ions has increased due to their back conversion via $BaO^+ + CO \rightarrow Ba^+ + CO_2$. The dashed lines are guides that show where the new Ba^+ ions are located.

D. Chemical reaction between BaO^+ and CO

Finally, the exothermic reaction $BaO^+ + CO \rightarrow Ba^+ + CO_2$ was studied in two different ways. The BaO^+ ions in their electronic ground state (their internal population is expected to be in equilibrium with the blackbody radiation environment at 300 K [39]), formed via chemical reactions, are not visible to the CCD camera. Therefore, we have observed the variation of shape of the ion crystal containing a certain

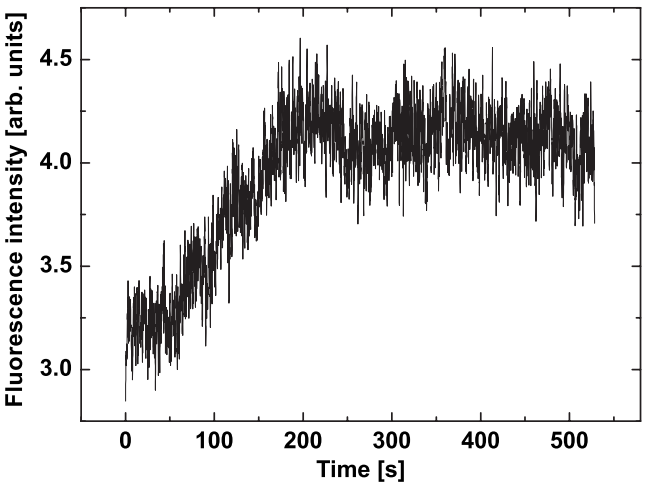

FIG. 12. Time evolution of the fluorescence intensity of the Ba^+ ion crystal shown in Fig. 11. The fluorescence intensity is proportional to the Ba^+ ion number and can be used to deduce the reaction rate constant, as described in the text. After approximately 200 s the observed fluorescence intensity and, thus, the Ba^+ ion number remains constant, due to the competing (loss) reaction channel between Ba^+ and neutral O_2 and CO_2 (see above).

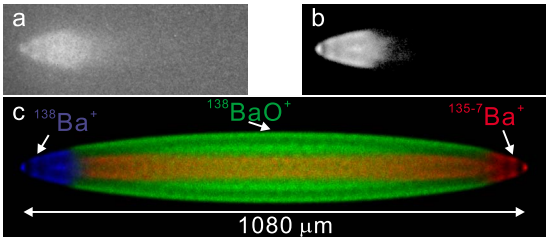

FIG. 13. (Color online) Efficiency of sympathetic cooling. CCD camera image (a) and MD simulations (b),(c) of the ion crystal in Fig. 6 after exposure to CO_2 for 66 min (at a pressure of 4×10^{-9} mbar). The ion ensemble contains 20 $^{138}Ba^+$, 120 SC barium isotopes ($^{135-137}Ba^+$), and 430 $^{138}Ba^{16}O^+$ ions. The temperature of each ion species is ≈25 mK. The simulated image in (b) shows the laser-cooled Ba^+ ions only, whereas the image in (c) shows all ion species contained in the crystal.

amount of BaO^+ ions when exposed to neutral CO gas, Fig. 11. Using the MD simulation, the decrease of the BaO^+ ion number and the corresponding increase in the $^{138}Ba^+$ ion number can be analyzed. Furthermore, the increase in the Ba^+ ion fluorescence intensity can be monitored (the latter being proportional to the number of $^{138}Ba^+$ ions in the crystal), Fig. 12. In both cases, we observe that the BaO^+ ions are not fully converted back to Ba^+ ions. This is most probably due to the fact that some of the Ba^+ ions react with residual O_2 (introduced to the vacuum chamber together with the CO gas) and CO_2 molecules (present in our vacuum system), leading to the formation of BaO^+ (see Figs. 1 and 6). Therefore, an equilibrium between Ba^+ formation and loss processes occurs.

E. Sympathetic cooling efficiency

The measurements described above also allow for a sensitive measurement of the sympathetic cooling efficiency. For this purpose, we have used chemical reactions between Ba^+ and neutral CO_2 in order to vary the ratio of sympathetically cooled to laser-cooled ions contained in the crystal systematically (Fig. 13). Initially, the barium ion crystal contained ≈450 $^{138}Ba^+$ and 120 SC barium isotopes. The temperature of each species was at ≈25 mK, comparable to the translational temperature of all ion crystals produced in this work. The final ion ensemble (after exposure to CO_2 gas for 66 min) contains 20 $^{138}Ba^+$, 120 SC barium isotopes, and 430 $^{138}Ba^{16}O^+$ ions. Sympathetic cooling works efficiently, even for ratios of sympathetically cooled to laser-cooled ion numbers as large as 27.5. This example also shows that using MD simulations, it is possible to accurately determine the ion numbers even for such crystals, by analyzing structural details of the part of the ion crystal visible to the CCD camera, as suggested in [36].

V. SUMMARY AND OUTLOOK

The results presented in this work represent a method for the production of cold trapped BaO^+ ions. It proceeds via laser-induced chemical reactions between cold trapped laser-excited Ba^+ ions and neutral molecular gases at room temperature. The method is efficient and allows for control of the number of produced BaO^+ molecular ions. The demonstration of this production extends the method demonstrated earlier on CaO^+ ions [22] to heavy diatomic molecular ions.

The ion ensembles produced were analyzed using MD simulations, which allows for a relatively precise determination of reaction rate constants. In particular, the ion species content and the shape of the ion crystals produced, detected via a CCD camera, were analyzed as a function of time after initiating the chemical reactions. The uncertainty in the determination of ion numbers via the simulations is below 5%.

The produced cold mixed-species ion crystals allowed for a study of the efficiency of sympathetic cooling. They show that cooling is very efficient even for ensembles where the fraction of laser-cooled ions is very small (<5%) compared to the fraction of sympathetically cooled ions. Such particular systems are of interest for extending the studies of the properties of multispecies ion crystals containing heavy ions. The cold trapped molecular ions (BaO^+) produced were used for further chemical reaction studies, in particular, their back conversion to Ba^+ ions via reaction with neutral CO.

Ion crystals containing heavy molecular ions are a good starting point for further investigations, such as cold chemical reactions with translationally and even internally cold neutral molecules (see [26]). Due to its relative simplicity, the production method based on chemical reactions may be applied to a variety of other species. The accuracy in the determination of ion numbers can be extended to the single-particle level, similar to the work in [19]. As a long-term perspective, chemical reaction studies may be extended to reactions between cold and heavy charged and neutral molecules prepared in specific quantum states, by using conventional laser techniques for internal state preparation [40], and to more complex molecular species, such as organic molecules interesting to chemistry and biology [27].

ACKNOWLEDGMENTS

The authors thank the Deutsche Forschungsgemeinschaft (DFG) and the EC network HPRN-CT-2002-00290 "Cold Molecules" for financial support. D.O. acknowledges support from the Studienstiftung des Deutschen Volkes and C.B.Z. from the Deutscher Akademischer Austauschdienst (DAAD).

[1] J. Doyle *et al.*, Eur. Phys. J. D **31**, 149 (2004).
[2] A. Fioretti, D. Comparat, A. Crubellier, O. Dulieu, F. Masnou-Seeuws, and P. Pillet, Phys. Rev. Lett. **80**, 4402 (1998).
[3] E. Hodby, S. T. Thompson, C. A. Regal, M. Greiner, A. C. Wilson, D. S. Jin, E. A. Cornell, and C. E. Wieman, Phys. Rev. Lett. **94**, 120402 (2005).
[4] S. Jochim *et al.*, Science **10**, 1126 (2003).
[5] C. A. Regal, C. Ticknor, J. L. Bohn, and D. S. Jin, Nature (London) **424**, 47 (2003).
[6] T. Kraemer *et al.*, Nature (London) **440**, 04626 (2006).
[7] J. D. Weinstein *et al.*, Nature (London) **395**, 148 (1998).
[8] F. M. H. Crompvoets, H. L. Bethlem, R. T. Jongma, and G. Meijer, Nature (London) **411**, 174 (2001).
[9] T. Rieger, T. Junglen, S. A. Rangwala, P. W.H. Pinkse, and G. Rempe, Phys. Rev. Lett. **95**, 173002 (2005).
[10] M. Wewer and F. Stienkemeier, Phys. Rev. B **67**, 125201 (2003).
[11] D. J. Larson, J. C. Bergquist, J. J. Bollinger, W. M. Itano, and D. J. Wineland, Phys. Rev. Lett. **57**, 70 (1986).
[12] M. D. Barrett *et al.*, Phys. Rev. A **68**, 042302 (2003).
[13] M. Drewsen, A. Mortensen, R. Martinussen, P. Staanum, and J. L. Sorensen, Phys. Rev. Lett. **93**, 243201 (2004).
[14] P. Blythe, B. Roth, U. Frohlich, H. Wenz, and S. Schiller, Phys. Rev. Lett. **95**, 183002 (2005).
[15] B. Roth, A. Ostendorf, H. Wenz, and S. Schiller, J. Phys. B **38**, 3673 (2005).
[16] A. Ostendorf, C. B. Zhang, M. A. Wilson, D. Offenberg, B. Roth, and S. Schiller, Phys. Rev. Lett. **97**, 243005 (2006).
[17] D. Offenberg *et al.* (unpublished).
[18] B. Roth, U. Fröhlich, and S. Schiller, Phys. Rev. Lett. **94**, 053001 (2005).
[19] B. Roth, P. Blythe, H. Wenz, H. Daerr, and S. Schiller, Phys. Rev. A **73**, 042712 (2006).
[20] B. Roth *et al.*, J. Phys. B **39**, S1241 (2006).
[21] L. Hornekær, Ph.D. thesis, Aarhus University, 2000.
[22] M. Drewsen *et al.*, in *Non-Neutral Plasma Physics IV*, edited by F. Anderegg, C. F. Driscoll, and L. Schweikhard, AIP Conf. Proc. No. 606 (AIP, Melville, NY, 2002), pp. 135–144.
[23] T. Baba and I. Waki, J. Chem. Phys. **116**, 1858 (2002).
[24] J. B. Hasted, *Physics of Atomic Collisions* (Butterworths, London, 1964).
[25] A. Bertelsen *et al.*, Eur. Phys. J. D **31**, 403–408 (2004).
[26] S. Willitsch, M. T. Bell, A. D. Gingell, S. R. Procter, and T. P. Softley, Phys. Rev. Lett. **100**, 043203 (2008).
[27] K. Hojbjerre, D. Offenberg, C. Z. Bisgaard, H. Stapelfeldt, P. F. Staanum, A. Mortensen, and M. Drewsen, Phys. Rev. A **77**, 030702(R) (2008).
[28] D. J. Larson, J. C. Bergquist, J. J. Bollinger, W. M. Itano, and D. J. Wineland, Phys. Rev. Lett. **57**, 70 (1986).
[29] M. G. Raizen, J. M. Gilligan, J. C. Bergquist, W. M. Itano, and D. J. Wineland, Phys. Rev. A **45**, 6493 (1992).
[30] E. Murad, J. Chem. Phys. **77**, 2057 (1982).
[31] A. Ostendorf, Ph.D. thesis, Duesseldorf University, 2006.
[32] K. P. Huber and G. Herzberg, *Molecular Spectra and Molecular Structure* (Van Nostrand Reinhold, New York, 1979).
[33] P. Bowe, L. Hornekaer, C. Brodersen, M. Drewsen, J. S. Hangst, and J. P. Schiffer, Phys. Rev. Lett. **82**, 2071 (1999).
[34] At temperatures above a few millikelvins, the case usually encountered experimentally, most ions in an ion crystal are not confined to particular sites, but diffuse between sites, due to their residual kinetic energy (determined by the cooling and heating conditions in the trap); see [37] for a detailed discussion. Because the CCD images show apparently individual spots, the ensembles seem crystallized, but are not. Except for special sites, the individual spots seen on the experimental images are not the positions where a particular single ion is confined, but where the probability to find any ion is high. Strictly speaking, it is thus erroneous (although usual) to denote ensembles at such temperatures as crystallized. "Structured liquids" may be a more appropriate description.
[35] The most important overall feature of crystallized mixed-species ion ensembles is a radial separation of the species due to their different effective trap potential (pseudopotential) strength. The effective trap potential U_{trap} for a particular ion species with charge Q and mass m scales as Q^2/m. In addition, for two ion species with charges Q_1 and Q_2, the interspecies intercation is $\sim Q_1 Q_2$. Thus, for equal charge of all ions, the total potential energy will usually be minimized if the lighter ions are closer to the axis. A radial gap between the species develops. For arbitrary charge ratio, in the limit of cylindrical symmetry (very prolate ensembles), the ratio of outer radius r_1 of the lower mass-to-charge ratio (say m_1/Q_1) ensemble and inner radius r_2 of the higher mass-to-charge ratio (say m_2/Q_2) ensemble is given by $r_1/r_2=(Q_2 m_1/Q_1 m_2)^{1/2}$ [D. J. Wineland, in *Proceedings of the Cooling, Condensation, and Storage of Hydrogen Cluster Ions Workshop, Menlo Park, 1987*, edited by J. T. Bahns (Dayton University, Menlo Park, CA, 1987), p. 181].
[36] B. Roth, P. Blythe, and S. Schiller, Phys. Rev. A **75**, 023402 (2007).
[37] C. B. Zhang, D. Offenberg, B. Roth, M. A. Wilson, and S. Schiller, Phys. Rev. A **76**, 012719 (2007).
[38] P. B. Armentrout and J. L. Beauchamp, Chem. Phys. **48**, 315 (1980).
[39] J. C. J. Koelemeij, B. Roth, and S. Schiller, Phys. Rev. A **76**, 023413 (2007).
[40] I. S. Vogelius, L. B. Madsen, and M. Drewsen, Phys. Rev. Lett. **89**, 173003 (2002).